

Learning Tensor Latent Features

Sung-En Chang
Northeastern
University

Xun Zheng
Carnegie Mellon
University

Ian E.H. Yen
Snap Inc.

Pradeep Ravikumar
Carnegie Mellon
University

Rose Yu
Northeastern
University

We study the problem of learning latent feature models (LFMs) for tensor data commonly observed in science and engineering such as hyperspectral imagery. However, the problem is challenging not only due to the non-convex formulation, the combinatorial nature of the constraints in LFMs, but also the high-order correlations in the data. In this work, we formulate a tensor latent feature learning problem by representing the data as a mixture of high-order latent features and binary codes, which are memory efficient and easy to interpret. To make the learning tractable, we propose a novel optimization procedure, **Binary Matching Pursuit** (BMP), that iteratively searches for binary bases via a MAXCUT-like boolean quadratic solver. Such procedure is guaranteed to achieve an ϵ -suboptimal solution in $O(1/\epsilon)$ greedy steps, resulting in a trade-off between accuracy and sparsity. When evaluated on both synthetic and real datasets, our experiments show superior performance over baseline methods.

1 Introduction

Latent feature models [11] (LFMs) are a family of unsupervised models that describe an observation as a combination of continuous valued latent *features* and binary valued sparse *codes*:

$$\mathbf{x} = \mathbf{W}^T \mathbf{z} + \mathbf{e}, \quad \mathbf{x} \in \mathbb{R}^M, \mathbf{W} \in \mathbb{R}^{R \times M}, \mathbf{z} \in \{0, 1\}^R.$$

Thus, for a given observation \mathbf{x} , its corresponding sparse code $\mathbf{z} \in \{0, 1\}^R$ indicates the presence or absence of latent features corresponding to the R rows of \mathbf{W} . Latent feature models have been widely studied

in the context of blind signal separation [26], overlapping clustering [2] and modeling natural image patches [16]. Compared to the classic latent factor models [14], latent feature models have two main benefits: (1) *interpretability*: the binary codes directly reveal whether certain features exist in the data, thus provide more interpretable latent profiles [25]; (2) *scalability*: compared with real-valued codes, binary codes require fewer bits to store, thereby cutting down the memory footprint, making it easier to deploy into memory constrained environments such as mobile devices.

Tensor latent feature models generalize traditional matrix latent feature models to represent high-order correlation structures in the data. For example, in spatiotemporal recommender systems, the observations are user activities over different locations and time. We want to learn the latent features and codes that correspond to user, space and time simultaneously without assuming conditional independence of these three dimensions. In this case, we can first represent such data as a high-order tensor and assign binary codes encoding presence or absence of rows for individual modes of the tensor. These codes can then help us answer the “when” and “where” questions regarding the learned user preferences.

Besides the non-convex formulation of the maximum likelihood estimation (MLE) objective, learning latent feature models is further complicated by the combinatorial nature of the codes. Inference of LFM from data is generally intractable. [24, 1, 12] propose spectral methods to bypass the issue of MLE objective. Although spectral methods provide global guarantees for the estimator, they usually have high sample complexity. Most recently, [29] proposed a solver based on convex relaxation that achieves linear sample complexity w.r.t number of atoms and dimensions, but is only limited to matrix LFMs. To learn a tensor model with integer components, [19] assumes all the components are integral and propose to use hierarchical alternating least square (ALS) to fit the integral codes for each mode iteratively. However, ALS is numerically unstable and susceptible to local optimum solutions [6], and

furthermore lacks theoretical guarantees.

In this paper, we propose an extension to latent feature models: Tensor Latent Feature Models for high-order data, which represent the data as a combination of high-order features and a set of binary codes. We first formulate a non-convex optimization problem corresponding to a MLE estimator. We then propose a novel optimization algorithm based on greedy matching pursuit to iteratively select atoms of steepest descent, by reduction the atom search problem to a MAXCUT problem amenable to efficient boolean quadratic solver. In summary, our contributions include:

- We study latent variable models for high-order data and formulate a tensor latent feature learning as a problem of convex objective with atomic sparsity constraint.
- Then we design a fast optimization algorithm based on greedy matching pursuit and MAXCUT-like Boolean quadratic subproblems to solve the problem efficiently with approximation guarantee.
- We theoretically analyze our algorithm and show that, to approximate an optimal solution of \bar{K} atoms, the algorithm achieves ϵ -suboptimal loss with $O(\bar{K}/\epsilon)$ number of atoms.
- We experiment exhaustively on synthetic and real-world benchmark datasets and observe superior performance for denoising and recovery tasks.

Notations Across the paper, we use calligraphy font for tensors, such as \mathcal{X}, \mathcal{Y} , bold uppercase letters for matrices, such as \mathbf{X}, \mathbf{Y} , and bold lowercase letters for vectors, such as \mathbf{x}, \mathbf{y} . For an L -mode tensor $\mathcal{X} \in \mathbb{R}^{I_1 \times \dots \times I_L}$, a generalized tensor unfolding $\mathbf{X} = \text{unfold}_S(\mathcal{X})$ w.r.t. a mode subset $S \subseteq \{I_1, \dots, I_L\}$ results in a matrix $\mathbf{X} \in \mathbb{R}^{S \times S^c}$ where the cyclic concatenation of modes S is treated as the first dimension and the cyclic concatenation of the rest are treated as the second dimension. Here, and in the sequel, we use a slight abuse of notation and use \mathbb{R}^S to indicate $\mathbb{R}^{\prod_{j \in S} I_j}$, and correspondingly for $\mathbb{R}^{S \times S^c}$. The reverse operation $\mathcal{X} = \text{refold}_S(\mathbf{X})$ is defined similarly. The indexing follows the convention in [13].

2 Related Work

Latent feature models. Our work is related to estimating latent feature models. For the non-parametric setting with Indian Buffet Process(IPB) prior, many [11, 8, 4] have studied estimation procedures based on Markov Chain Monte Carlo (MCMC)

[8] or variational inference [7]. For the parametric version of the model, [24, 1, 12] propose to use spectral methods to estimate the moments of the distribution at different orders, but can suffer from high sample complexity. Under certain identifiability condition, [21] proposed a convex optimization algorithm by selecting a maximal affine independent subset. However, the selection process in their algorithm has an exponential computational complexity. Perhaps the work that is most related to ours is [29] in which a convex estimator for matrix latent feature models which under certain identifiability conditions achieves a linear sample complexity.

Tensor decomposition. Tensor decomposition has been the subject of extensive study; please see the review paper by [13] and references therein. Most tensor factorization work focuses on extracting high-order structure with real-value components. Due to the non-convex nature of low-rank tensors, [9, 22] propose to use n -mode nuclear norm as a convex surrogate and solve the problem using alternating direction method of multipliers (ADMM). Solving convex surrogates have global guarantees but can suffer from high computational costs. [30] designed a non-convex solver based on greedy matching pursuit and demonstrate significant speedup. There has also been work on binary tensor decomposition where the input tensor has binary values [17, 20], which is different from our problem where the learned components are binary. [19] have a similar formulation of the problem but propose a heuristic based on alternating least squares. To the best of our knowledge, our work is the first algorithm for learning tensor decomposition with binary components with theoretical guarantees.

3 Learning Tensor Latent Features

In this section, we first review the background of matrix LFM and describe their extension to tensors, aka tensor latent feature models. We then formulate the tensor LFM learning problem as sparsity constrained convex minimization on an atomic set.

3.1 Matrix Latent Feature Model

In the regime of latent variable modeling, popular choices include mixture models which assume each data sample $\mathbf{x} \in \mathbb{R}^M$ is represented by a single latent class. Latent feature models [11] generalizes mixture models by assuming each sample to come from a combination of latent features, resulting the following data generation process:

$$\mathbf{x} = \mathbf{W}^T \mathbf{z} + \mathbf{e}, \quad (1)$$

where $\mathbf{W} \in \mathbb{R}^{R \times M}$ is a set of R latent features, $\mathbf{z} \in \{0, 1\}^R$ is a latent binary vector that indicates the presence or absence of each feature. $\mathbf{e} \in \mathbb{R}^M$ is the unknown noise vector with mean zero. LFM are used to model matrix data and assume linear correlations among features.

3.2 Tensor Latent Feature Model

To model tensor data with high-order non-linear correlations, we generalize LFM to tensor latent feature models. In particular, let $\mathcal{X} \in \mathbb{R}^{I_1 \times \dots \times I_L}$ be a general L -mode data tensor, and $S \subseteq [L]$ be a subset of the modes. Let π be a set of different partitions of the modes $[L]$, i.e. a collection of pairs (S, S^c) specified by the user. This allows us to choose the modes where the high-order correlations exist.

Tensor latent feature models assume each observation to be represented by a set of latent *tensor features* and a binary vector of codes indicating the presence of the features. Specifically, we impose the following latent feature structure to the tensor:

$$\mathcal{X} = \sum_{(S, S^c) \in \pi} \sum_{\mathbf{z} \in \{0, 1\}^S, \mathbf{w} \in \mathbb{R}^{S^c}} \text{refold}_S(\mathbf{z} \mathbf{w}^T) + \mathcal{E}, \quad (2)$$

where \mathcal{E} is the unknown noise tensor whose elements are drawn i.i.d from a zero mean distribution. For each mode subset S , the corresponding basis tensor is a folded rank-1 matrix consists of a binary code vector \mathbf{z} and a real-valued feature vector \mathbf{w} .

The imposed structure in Eqn. 2 generalizes the matrix LFM model not only by extending from a 2-dimensional array to the multi-dimensional setting, but also by allowing all specified partitions of modes that can be explained by binary combination of features. One can also draw an analogy from the dirty statistical model [28], which aims to learn multiple different correlation structures of the data simultaneously, e.g. sparsity and low-rankness. In the tensor latent feature model, each partition of the modes can be seen as a *clean* statistical model that promotes a particular low-rank structure, and the combination of such partitions is leads to a *dirty* statistical model.

3.3 Reformulating via Atomic Set

The estimation (learning) problem of tensor latent feature models in Eqn. 2 is generally intractable: searching for latent features and binary codes leads to a hard non-convex optimization problem with combinatorial constraints. In addition, general mixed integer program solvers are not applicable due to the real-valued features \mathbf{w} . To make the learning tractable, we reformulate the regularized MLE estimation problem

as sparsity constrained convex minimization using an atomic set.

To begin with, let us define a set of atoms given a mode subset S :

$$\mathbb{A}_S = \{ \text{refold}_S(\mathbf{z} \mathbf{v}^T) \mid \mathbf{z} \in \{0, 1\}^S, \mathbf{v} \in \mathbb{S}^{S^c} \}$$

where \mathbb{S}^p is a unit sphere in \mathbb{R}^p , hence we use \mathbf{v} instead of \mathbf{w} to make this change explicit. Then the atom sets for all the partitions is

$$\mathbb{A} = \bigcup_{(S, S^c) \in \pi} \mathbb{A}_S.$$

Now every real-valued features is a unit vector, and we can associate each “unit” basis tensor \mathcal{M} with a real-valued coefficient $c_{\mathcal{M}}$:

$$\mathbf{c} = \{c_{\mathcal{M}} \mid \mathcal{M} \in \mathbb{A}\}, \quad (3)$$

For the tensor latent feature learning problem, given an observation $\mathcal{X} \in \mathbb{R}^{I_1 \times \dots \times I_L}$ generated from the model (2), we would like to find a most compact representation of \mathcal{X} in the space of \mathbb{A} . We can then write the learning problem as the following convex minimization problem with non-convex sparsity constraints over the atom set:

$$\begin{aligned} \min_{\mathcal{W}} \quad & F(\mathcal{W}) := \frac{1}{2} \|\mathcal{X} - \mathcal{W}\|_F^2 \\ \text{s.t.} \quad & \mathcal{W} = \sum_{\mathcal{M} \in \mathbb{A}} c_{\mathcal{M}} \mathcal{M}, \quad \|c\|_0 \leq \bar{K}, \end{aligned} \quad (4)$$

where $\|\mathcal{W}\|_F = \sqrt{\sum_{i_1, \dots, i_L} \mathcal{W}_{i_1, \dots, i_L}^2}$ is the tensor Frobenius norm, and \bar{K} is the desired number of atoms from the atom set \mathbb{A} .

4 Binary Matching Pursuit (BMP)

Solving problem in Eqn. (4) is still difficult as the atomic set contains an immensely large number of atoms. In this section, we introduce Binary Matching Pursuit (BMP), a binary variant of the classic matching pursuit algorithm with an efficient MAXCUT-like Boolean quadratic solver as a subroutine. The algorithms are outlined in Algorithm 1 and Algorithm 2.

4.1 Greedy Matching Pursuit

Matching pursuit [15, 23] is a sparse approximation algorithm that aims to find the “best match” of the data onto a span of basis. Similar to matching pursuit, we first perform a linearization of the objective. In particular, at iteration k , we greedily find a basis

Algorithm 1 BinaryMatchingPursuit

```

1: Input: Tensor  $\mathcal{X}$ 
2: Output: Tensor  $\mathcal{W}$ 
3: Initialize  $\mathcal{W}^0 \leftarrow 0$ , active set  $A^0 \leftarrow \emptyset$ 
4: for  $k \leftarrow 1, \dots, K$  do
5:   Atom  $\mathcal{M}^* \leftarrow \text{GreedyAtomSearch}(\mathcal{X}, \mathcal{W}^{k-1})$ 
6:   Add to active set  $A^k \leftarrow A^{k-1} \cup \{\mathcal{M}^*\}$ 
7:   Adjust weights  $\mathbf{c}$  by solving (11)
8:   Reconstruct  $\mathcal{W}^k \leftarrow \sum_{\mathcal{M} \in A^k} c_{\mathcal{M}} \mathcal{M}$ 

```

$\mathcal{M}^* \in \mathbb{A}$ that corresponds to the steepest gradient descent direction.

$$\mathcal{M}^* = \operatorname{argmin}_{\mathcal{M} \in \mathbb{A}} \langle \nabla F(\mathcal{W}^k), \mathcal{M} \rangle. \quad (5)$$

Since we know the partition set π , the greedy step is in fact solving a nested minimization problem:

$$\min_{(S, S^c) \in \pi} \min_{\mathcal{M} \in \mathbb{A}_S} \langle \nabla F(\mathcal{W}^k), \mathcal{M} \rangle. \quad (6)$$

The difficulty in solving (6) lies in the fact that the inner optimization problem over the atom set involves a combinatorially large number of atoms. A key contribution of this work is a novel procedure based on a MAXCUT like Boolean quadratic solver to tackle this problem efficiently.

For ease of illustration, assume that $\nabla F(\mathcal{W})$ is already unfolded into a $p \times q$ matrix, where $p = \prod_{j \in S} I_j$ and $q = \prod_{j \in S^c} I_j$. Then each inner minimization problem in Eqn. (6) can be written as

$$\min_{\mathbf{z} \in \{0,1\}^p, \mathbf{v} \in \mathbb{S}^q} \langle \nabla F(\mathcal{W}^k), \mathbf{z} \mathbf{v}^T \rangle. \quad (7)$$

Since the feature vector \mathbf{v} lies in the space of real-valued unit vectors, when fixing \mathbf{z} and minimizing w.r.t. \mathbf{v} , we have

$$\mathbf{v}^*(\mathbf{z}) = \frac{\nabla F(\mathcal{W}^k)^T \mathbf{z}}{\|\nabla F(\mathcal{W}^k)^T \mathbf{z}\|}$$

Therefore, the joint minimization w.r.t. (\mathbf{z}, \mathbf{v}) is equivalent to solving

$$\begin{aligned} \mathbf{z}^* &= \operatorname{argmin}_{\mathbf{z} \in \{0,1\}^p} \mathbf{z}^T \underbrace{\nabla F(\mathcal{W}^k) \nabla F(\mathcal{W}^k)^T}_{-C} \mathbf{z} \\ &= \operatorname{argmax}_{\mathbf{z} \in \{0,1\}^p} \mathbf{z}^T C \mathbf{z}. \end{aligned} \quad (8)$$

which can be solved using a Boolean quadratic solver efficiently, as detailed in the next section.

4.2 Boolean Quadratic Solver via MAXCUT

With change of variables, it has been shown that the problem in Eqn 8 is a MAXCUT-like problem [29],

Algorithm 2 GreedyAtomSearch

```

1: Input: Tensor  $\mathcal{X}, \mathcal{W}$ 
2: Output: Atom  $\mathcal{M}^*$ 
3: for each partition  $(S, S^c) \in \pi$  do
4:   Gradient  $G \leftarrow \text{unfold}_S(\nabla F(\mathcal{W}))$ 
5:   Quadratic term  $C \leftarrow -GG^T$ 
6:   Solve MAXCUT  $\mathbf{z} \leftarrow \text{MaxCut}(C)$ 
7:   Unit vector  $\mathbf{v} \propto G^T \mathbf{z}$ 
8:   Candidate atom  $\mathcal{M}_S \leftarrow \text{refold}_S(\mathbf{z} \mathbf{v}^T)$ 
9: Greedy  $\mathcal{M}^* \leftarrow \operatorname{argmin}_{\{\mathcal{M}_S\}} \langle \nabla F(\mathcal{W}), \mathcal{M}_S \rangle$ .

```

which has an efficient relaxation with constant approximation guarantee.

Specifically, define a vector $\mathbf{y} = 2\mathbf{z} - 1$, then $\mathbf{y} \in \{-1, 1\}^p$. Augmented with another dummy variable $y_0 \in \{-1, 1\}$, the problem can be rewritten as

$$\max_{[y_0; \mathbf{y}] \in \{-1, 1\}^{p+1}} \frac{1}{4} \begin{bmatrix} y_0 \\ \mathbf{y} \end{bmatrix}^T \underbrace{\begin{bmatrix} \mathbf{1}^T C \mathbf{1} & \mathbf{1}^T C \\ C \mathbf{1} & C \end{bmatrix}}_{\tilde{C}} \begin{bmatrix} y_0 \\ \mathbf{y} \end{bmatrix}, \quad (9)$$

which is now in a MAXCUT-like formulation. In general, even if the quadratic factor is positive definite, i.e., $\tilde{C} \succ 0$, the decision version of the problem is still NP-complete [10]. However, there exist semidefinite programming (SDP) relaxations that has constant factor approximation guarantees [18]:

$$\begin{aligned} \max_{Y \succeq 0} \quad & \langle \tilde{C}, Y \rangle \\ \text{s.t.} \quad & \operatorname{diag}(Y) = \mathbf{1}, \end{aligned} \quad (10)$$

Rounding of the solution to the above SDP problem guarantees a 3/5-approximation [18, 29].

Indeed, although the polynomial time complexity of SDPs is already a big saving compared to NP-completeness, it is still impractical to employ a general SDP solver as the subroutine. Fortunately, unlike general SDPs, the SDP of the form (10) has specialized solver [27], whose time complexity only depends linearly on the number of non-zeros in \tilde{C} .

4.3 Weight Adjustment

After obtaining an atom \mathcal{M}^* using the Boolean quadratic solver, we can add the atom to the current atom set A^k that maintains active atoms considered so far. The next step is to adjust the atom weights to reflect changes in the atom set. Let $|A^k|$ be the number of active atoms at iteration k . Fixing the atom set A^k , we can rewrite (4) in terms of \mathbf{c} as:

$$\min_{\mathbf{c} \in \mathbb{R}^{|A^k|}} \frac{1}{2} \|\mathcal{X} - \sum_{\mathcal{M} \in A^k} c_{\mathcal{M}} \mathcal{M}\|_F^2, \quad (11)$$

which is a simple least-square problem with a closed-form solution:

$$\mathbf{c} = (M^T M)^{-1} M^T \text{vec}(\mathcal{X}) \quad (12)$$

where M is a $\dim(\mathcal{X}) \times |A^k|$, each column of which is a flattened atom $\text{vec}(\mathcal{M})$ in the active set A^k .

5 Convergence Analysis

In this section, we show that the greedy algorithm proposed in section 4 leads to an accuracy-sparsity trade-off: by running the algorithm for $\Omega(\bar{K}/\epsilon)$ iterations, one can achieve an ϵ -suboptimal loss relative to the optimal solution of (4) with \bar{K} number of atoms.

A key ingredient of our analysis is the $\mu = 3/5$ constant-approximation guarantee in the greedy step given by the SDP-based MAXCUT solver, where we have the following guarantee for the atom \mathcal{M}^* picked by Algorithm 2:

$$\langle \nabla F(\mathcal{W}), \mathcal{M}^* \rangle \leq \mu \left(\min_{\mathcal{M} \in \mathbb{A}} \langle \nabla F(\mathcal{W}), \mathcal{M} \rangle \right). \quad (13)$$

The definition of *atomic norm* [5] will be useful in the analysis:

$$\|\mathcal{W}\|_{\mathbb{A}} = \left\{ \inf \|\mathbf{c}\|_1 : \mathcal{W} = \sum_{\mathcal{M} \in \mathbb{A}} c_{\mathcal{M}} \mathcal{M} \right\}. \quad (14)$$

Theorem 5.1. *Let \mathcal{W}^* be the optimal solution of problem (4). The iterates $\{\mathcal{W}^k\}_{k=1}^K$ given by the BMP Algorithm 1 satisfies*

$$F(\mathcal{W}^k) - F(\mathcal{W}^*) \leq \frac{2\beta\|\mathcal{W}^*\|_{\mathbb{A}}^2}{\mu^2} \left(\frac{1}{k} \right) \quad (15)$$

Proof. Denote

$$\text{span}(A) = \{ \mathcal{W} \mid \mathcal{W} = \sum_{\mathcal{M} \in A} c_{\mathcal{M}} \mathcal{M}, \mathbf{c} \in \mathbb{R}^{|A|} \}$$

and

$$\Delta\mathcal{W}_{\perp} := \text{proj}_{\text{span}(A^{k-1})^{\perp}}(\Delta\mathcal{W}).$$

By the fully-corrective weight adjustment (11), for each iteration k we have

$$F(\mathcal{W}^{k+1}) = \min_{\mathcal{W} \in \text{span}(A^k)} F(\mathcal{W}) \leq \min_{c \in \mathbb{R}} F(\mathcal{W}^k + c\mathcal{M}_{\perp}^*)$$

since $\mathcal{W}^k + c\mathcal{M}_{\perp}^* \in \text{span}(A^k)$. Let β be the Lipschitz-continuous parameter of $\nabla F(\mathcal{W})$ w.r.t. the atomic norm $\|\mathcal{W}\|_{\mathbb{A}}$. We have

$$F(\mathcal{W} + \Delta\mathcal{W}) - F(\mathcal{W}) \leq \langle \nabla F(\mathcal{W}), \Delta\mathcal{W} \rangle + \frac{\beta}{2} \|\Delta\mathcal{W}\|_{\mathbb{A}}^2$$

for any $\Delta\mathcal{W}$, and therefore

$$\begin{aligned} & F(\mathcal{W}^{k+1}) - F(\mathcal{W}^k) \\ & \leq \min_c \langle \nabla F(\mathcal{W}^k), c\mathcal{M}_{\perp}^* \rangle + \frac{\beta}{2} \|c\mathcal{M}_{\perp}^*\|_{\mathbb{A}}^2. \end{aligned} \quad (16)$$

Note since $\langle \nabla F(\mathcal{W}^k), \Delta\mathcal{W} \rangle = 0$ for any $\Delta\mathcal{W} \in \text{span}(A^{k-1})$, we also have

$$\begin{aligned} & \min_c \langle \nabla F(\mathcal{W}^k), c\mathcal{M}_{\perp}^* \rangle + \frac{\beta}{2} \|c\mathcal{M}_{\perp}^*\|_{\mathbb{A}}^2 \\ & = \min_{\Delta\mathcal{W} \in \text{span}(A^{k-1})^{\perp}} \mu \langle \nabla F(\mathcal{W}^k), \Delta\mathcal{W} \rangle + \frac{\beta}{2} \|\Delta\mathcal{W}_{\perp}\|_{\mathbb{A}}^2 \\ & = \min_{\Delta\mathcal{W} \in \text{span}(\mathbb{A})} \mu \langle \nabla F(\mathcal{W}^k), \Delta\mathcal{W} \rangle + \frac{\beta}{2} \|\Delta\mathcal{W}_{\perp}\|_{\mathbb{A}}^2 \\ & \leq \min_{\Delta\mathcal{W} = \alpha(\mathcal{W}^* - \mathcal{W}^k), \alpha \in [0, 1]} \mu \langle \nabla F(\mathcal{W}^k), \Delta\mathcal{W} \rangle + \frac{\beta}{2} \|\Delta\mathcal{W}_{\perp}\|_{\mathbb{A}}^2 \\ & \leq \min_{\alpha \in [0, 1]} \alpha \mu(F(\mathcal{W}^*) - F(\mathcal{W}^k)) + \frac{\beta\alpha^2}{2} \|\mathcal{W}_{\perp}^*\|_{\mathbb{A}}^2 \end{aligned}$$

where the first inequality is due to $\alpha(\mathcal{W}^* - \mathcal{W}^k) \in \text{span}(\mathbb{A})$, and the second inequality is from convexity. Let $F^* := F(\mathcal{W}^*)$. Combining the above inequality with (16), we have

$$\begin{aligned} & (F(\mathcal{W}^{k+1}) - F^*) - (F(\mathcal{W}^k) - F^*) \\ & \leq -\max \left\{ \frac{\mu^2}{2\beta\|\mathcal{W}^*\|_{\mathbb{A}}^2} (F(\mathcal{W}^k) - F^*)^2, \frac{\mu}{2} (F(\mathcal{W}^k) - F^*) \right\} \end{aligned}$$

The recurrence then leads to the convergence result. \square

Consider an optimal solution with support \bar{A} of size \bar{K}

$$\mathcal{W}^* = \sum_{\mathcal{M} \in \bar{A}} c_{\mathcal{M}}^* \mathcal{M}.$$

Based on Theorem 5.1, we develop a bound on the optimization error directly in terms of the ratio \bar{K}/K where K is the number of atoms selected by our algorithm.

Theorem 5.2. *Let γ be the strongly-convex parameter of the function $f(\mathbf{c}) := F(\sum_{\mathcal{M} \in \bar{A}} c_{\mathcal{M}} \mathcal{M})$. Then the loss obtained from running \bar{K} iterates of Algorithm 1 satisfies*

$$F(\mathcal{W}^{\bar{K}}) - F(\mathcal{W}^*) \leq \frac{2\beta\|\mathcal{X}\|_F^2}{\gamma\mu^2} \left(\frac{\bar{K}}{K} \right) \quad (17)$$

Proof. Since \mathbf{c}^* is the minimizer of $f(\mathbf{c})$, it satisfies $\langle \nabla f(\mathbf{c}^*), \mathbf{c}^* \rangle = 0$ and thus

$$\begin{aligned} f(0) - f(\mathbf{c}^*) &= f(0) - f(\mathbf{c}^*) - \langle \nabla f(\mathbf{c}^*), 0 - \mathbf{c}^* \rangle \\ &\geq \frac{\gamma}{2} \|\mathbf{c}^*\|^2. \end{aligned}$$

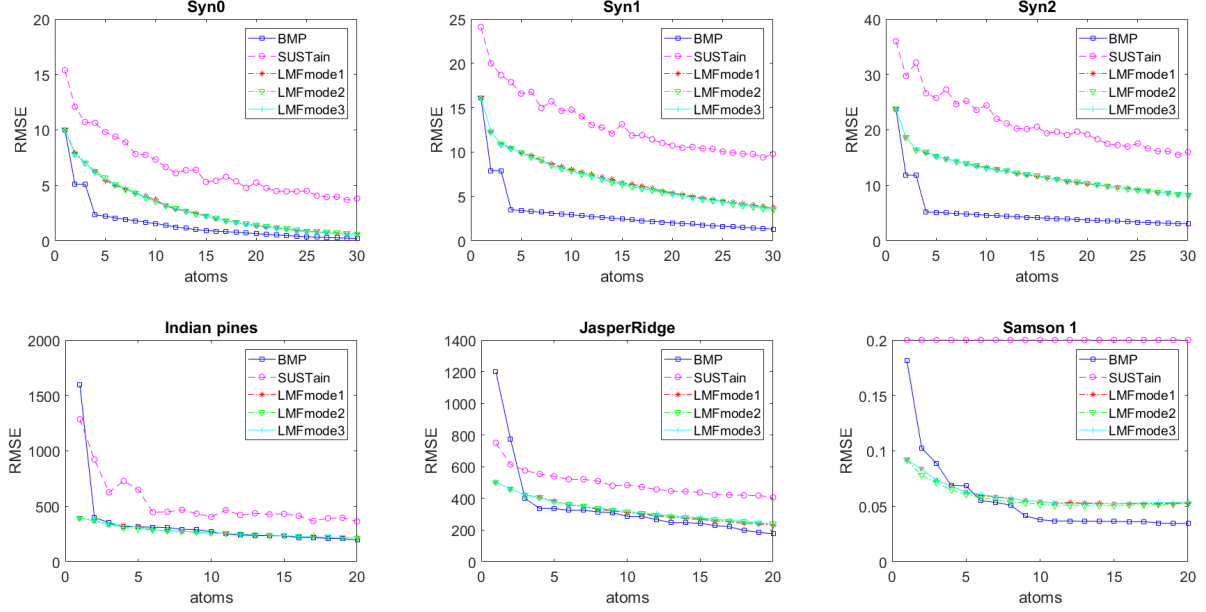


Figure 1: Denoising: RMSE (lower is better) vs number of atoms. (Top row) Synthetic data. (Bottom row) Real data. BMP achieves better RMSE in nearly all settings.

Since, $f(0) - f(\mathbf{c}^*) \leq \frac{1}{2} \|\mathcal{X}\|_F^2$, we have

$$\|\mathcal{W}^*\|_{\mathbb{A}}^2 = \|\mathbf{c}^*\|_1^2 \leq \bar{K} \|\mathbf{c}^*\|_2^2 \leq \frac{\bar{K} \|\mathcal{X}\|_F^2}{\gamma}. \quad (18)$$

Substituting (18) into (15) yields the result (17). \square

6 Experiments

We evaluate our method on two benchmark tasks for latent feature modeling in the context of tensors: tensor denoising and tensor recovery. For denoising, we assume that the observations \mathcal{X} are contaminated by element-wise Gaussian noise, and the task is to filter out the noise. For recovery, the data \mathcal{X} have randomly missing values, and the task is to recover these missing entries solely based on observed ones.

Baselines. SUSTain [19] solves the following integer tensor factorization problem for observation $\mathcal{X} = \mathbb{R}^{I_1 \times \dots \times I_L}$:

$$\begin{aligned} \min_{\mathbf{c}, \{M^{(l)}\}, \mathcal{W}} \quad & \frac{1}{2} \|\mathcal{X} - \mathcal{W}\|_F^2 \\ \text{s.t.} \quad & \mathcal{W} = \sum_{r=1}^R c_r M^{(1)}(:, r) \circ \dots \circ M^{(L)}(:, r) \\ & c_r \in \mathbb{Z}_+, \quad M^{(l)} \in \mathbb{Z}_{\tau}^{I_l \times R} \end{aligned} \quad (19)$$

where \circ denotes outer product, \mathbb{Z}_+ is the set of non-negative integers, and $\mathbb{Z}_{\tau} = \{0, 1, \dots, \tau\}$ is the set of

nonnegative integers up to τ . We use a publicly available implementation ¹ and the default parameter settings provided in the repository. For our experiments, we set $\tau = 1$ and run SUSTain to generate binary components. We note that with this setting, SUSTain constrains all the tensor components to be binary, which is a stronger assumption than ours. Therefore the results presented in this experiment is not necessarily indicative of SUSTain's performance on general integer tensor factorization problems.

We also compare with matrix latent feature models (LFMs) in order to demonstrate the benefit of exploiting high-order structures. Specifically, we unfold the input tensor \mathcal{X} w.r.t. each mode separately, resulting a set of unfolded matrices. For each mode, we have the input matrix $\mathbf{X} = \text{unfold}_S(\mathcal{X})$ where $S = \{l\}$ for each $l \in [L]$. We use LFM mode l to denote applying LFM to the unfolding matrix of mode l .

Datasets. We use three synthetic and three real-world datasets. For synthetic dataset, we set $L = 3$, $I_1 = I_2 = 100$, and $I_3 = 10$. The ground truth tensor \mathcal{X}^* with K atoms is generated as follows. For each atom $k \in [K]$, let $l = k \bmod L$ be the chosen mode. We generate a random binary vector $\mathbf{z}_l \in \{0, 1\}^l$ for the mode l , and generate two random real-valued vectors $\mathbf{w}_{l'} \in \{1, \dots, 5\}^{I_{l'}}$, $\mathbf{w}_{l''} \in \{1, \dots, 5\}^{I_{l''}}$ for the remaining modes l' and l'' . The k -th atom \mathcal{M}_k is then formed by taking outer products of \mathbf{z}_l , $\mathbf{w}_{l'}$, and $\mathbf{w}_{l''}$

¹<https://github.com/kperros/SUSTain/>

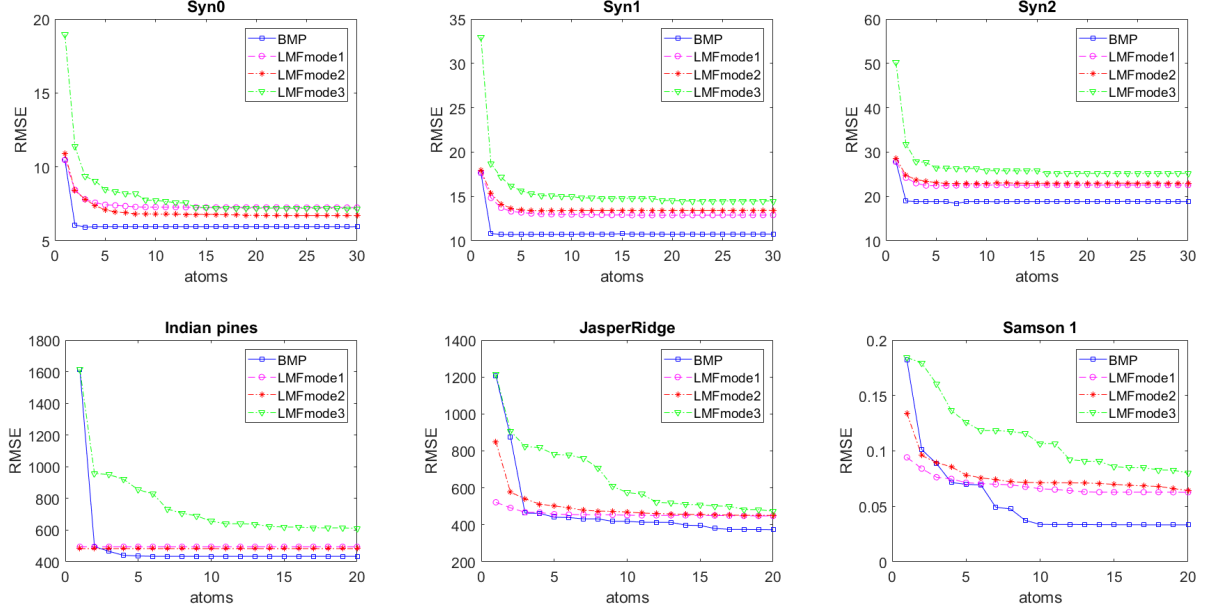


Figure 2: Recovery: RMSE (lower is better) vs number of atoms. (Top row) Synthetic data. (Bottom row) Real data. BMP consistently outperforms baselines in terms of RMSE.

in appropriate order. The final ground truth tensor is simply the summation of all atoms $\mathcal{X}^* = \sum_{k=1}^K \mathcal{M}_k$. We test on synthetic data sets with different number of atoms: $K \in \{6, 15, 30\}$, and call them **Syn0**, **Syn1**, and **Syn2** respectively.

We use the following three real-world hyperspectral image datasets: Indian pines (**Ind.**)², JasperRidge (**Jas.**)³, and Samson1 (**Sam.**)⁴. The Indian Pines dataset was gathered over the Indian Pines test site in northwestern Indiana and consists of 145×145 pixels and 224 spectral reflectance bands [3]. Jasper Ridge has 512×614 pixels, each of which is recorded at 224 channels ranging from 380 nm to 2500 nm. Samson has 952×952 pixels, each recorded at 156 channels covering the wavelengths ranging from 401 nm to 889 nm. Since this hyperspectral imagery is very large, we consider a sub-image of 100×100 for Jasper Ridge and 95×95 pixels for Samson, similar to [31, 32, 33]. The data sets statistics are summarized in the table below.

	Syn0	Syn1	Syn2	Ind.	Jas.	Sam.
row	100	100	100	145	100	95
col	100	100	100	145	100	95
bands	10	10	10	200	224	156

²http://www.ahu.eus/ccwintco/index.php?title=Hyperspectral_Remote_Sensing_Scenes
³http://www.escience.cn/people/feiyunZHU/Dataset_GT.html

⁴http://www.escience.cn/people/feiyunZHU/Dataset_GT.html

For both synthetic and real dataset, we set the partition as $\pi = \{(S_1, S_1^c), (S_2, S_2^c), (S_3, S_3^c)\}$, where $S_1 = \{1\}$, $S_2 = \{2\}$, and $S_3 = \{3\}$.

6.1 Tensor Denoising

For the denoising experiments, we generate noisy observations \mathcal{X} from a ground truth tensor \mathcal{X}^* using

$$\mathcal{X}_{ijk} = \mathcal{X}_{ijk}^* + e, \quad e \sim N(0, 0.1). \quad (20)$$

The goal is to filter out noise from the observed \mathcal{X} . For evaluation, we use root-mean-square error (RMSE) between the ground truth \mathcal{X}^* and the estimate \mathcal{W} :

$$\text{RMSE}(\mathcal{W}) = \sqrt{\frac{1}{I_1 I_2 I_3} \sum_{ijk} (\mathcal{X}_{ijk}^* - \mathcal{W}_{ijk})^2}. \quad (21)$$

The results are shown in Figure 1. The top row shows the comparison on three synthetic data sets where the true number of atoms are $K = 6, 15, 30$ respectively. One can observe that BMP achieves much better RMSE across different numbers of atoms compared to other baselines. The improvement over LFM baselines suggests the advantage of modeling high-order correlations using tensors. The comparison with fully binary-valued **SUSTain** confirms the advantage of real-valued factors in tensor latent feature models. We also notice that as the number of atoms increases, the advantage of our method becomes more pronounced.

The bottom row displays the denoising results on the hyperspectral imagery. Although initially on a limited

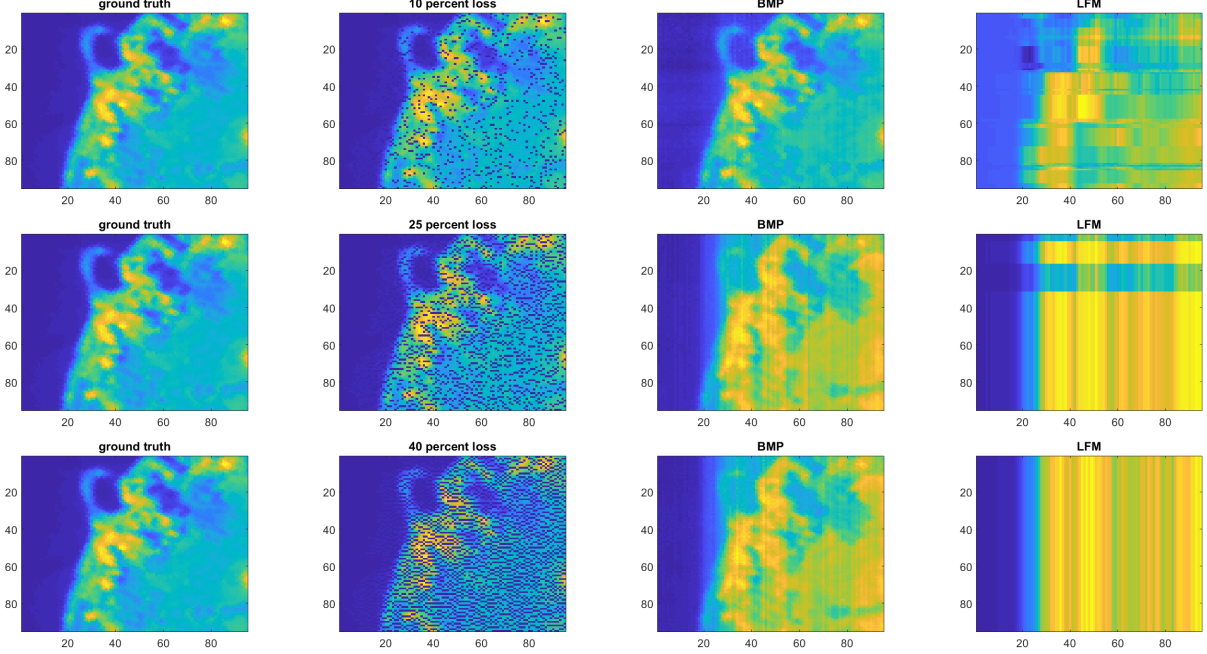


Figure 3: Recovery result on channel 138 of Samson data, with varying percentage of missing entries. Four columns are ground truth, partial observation, recovery with **BMP**, and recovery with **LFM** respectively. **BMP** recovery is better at recovering missing entries, showing the advantage of tensor latent feature model.

number of atoms **BMP** has a large RMSE, as the number of atoms grows, it quickly outperforms baseline methods. Also notice that for Indian Pines **BMP** achieves similar performance as **LFM**, whereas in Jasper Ridge and Samson dataset **BMP** significantly outperforms **LFM**.

6.2 Tensor Recovery

In the recovery task, we randomly remove 10, 25, and 40 percent of the entries from the ground truth tensor \mathcal{X}^* with the goal of repainting the missing entries from partial observations \mathcal{X} . We use RMSE between the ground truth \mathcal{M}^* and the estimate \mathcal{W} as above as the evaluation metric. Results using 10% missing entries are shown in Figure 2. On synthetic data (top row), **BMP** outperforms other baselines starting from 2 atoms. In the bottom row, even though **BMP** starts out similar to other methods, it achieves much better RMSE after 10 atoms. The trend is consistent in all settings where **BMP** outperforms other baselines, especially on the Samson dataset.

For a visual comparison, in Figure 3 we visualize the recovery results from channel 138 of the Samson1 dataset for different settings. In the first row, where 10% of the entries are missing, **BMP** can obtain a visually close estimate, whereas **LFM** only captures a rough picture of the data. In the second and third row, as more and more entries are missing, **BMP** can still robustly recover the selected channel, despite it not using

real-valued factorization. On the other hand, **LFM** performs poorly, suggesting again the advantage of tensor latent feature model over its matrix counterparts.

7 Conclusion

In this paper, we generalize the problem of learning latent feature models from matrix to tensor data. We define a flexible tensor latent feature model and formulate a tractable latent feature learning problem. We design a fast optimization algorithm to search for the binary atoms iteratively using greedy matching pursuit and a MAXCUT solver. We theoretically analyze our algorithm and prove it can achieve an ϵ -suboptimal loss relative to the optimal solution in $O(1/\epsilon)$ iterations. We experiment exhaustively on synthetic and real-world datasets and observe superior performance for both tensor denoising and recovery tasks.

References

[1] Animashree Anandkumar, Rong Ge, Daniel Hsu, Sham M Kakade, and Matus Telgarsky. Tensor decompositions for learning latent variable models. *The Journal of Machine Learning Research*, 15(1):2773–2832, 2014.

[2] Arindam Banerjee, Chase Krumpelman, Joydeep Ghosh, Sugato Basu, and Raymond J Mooney. Model-based overlapping clustering. In *Proceedings of the eleventh ACM SIGKDD international conference on Knowledge discovery in data mining*, pages 532–537. ACM, 2005.

[3] Marion F. Baumgardner, Larry L. Biehl, and David A. Landgrebe. 220 band aviris hyperspectral image data set: June 12, 1992 indian pine test site 3, Sep 2015.

[4] Tamara Broderick, Brian Kulis, and Michael Jordan. Mad-bayes: Map-based asymptotic derivations from bayes. In *International Conference on Machine Learning*, pages 226–234, 2013.

[5] Venkat Chandrasekaran, Benjamin Recht, Pablo A. Parrilo, and Alan S. Willsky. The Convex Geometry of Linear Inverse Problems. *Foundations of Computational Mathematics*, 2012.

[6] Andrzej Cichocki and Rafal Zdunek. Regularized alternating least squares algorithms for non-negative matrix/tensor factorization. In *International Symposium on Neural Networks*, pages 793–802. Springer, 2007.

[7] Finale Doshi, Kurt Miller, Jurgen Van Gael, and Yee Whye Teh. Variational inference for the indian buffet process. In *Artificial Intelligence and Statistics*, pages 137–144, 2009.

[8] Finale Doshi-Velez and Zoubin Ghahramani. Accelerated sampling for the indian buffet process. In *Proceedings of the 26th annual international conference on machine learning*, pages 273–280. ACM, 2009.

[9] Silvia Gandy, Benjamin Recht, and Isao Yamada. Tensor completion and low-n-rank tensor recovery via convex optimization. *Inverse Problems*, 27(2):025010, 2011.

[10] Michael R Garey and David S Johnson. Computers and intractability, a guide to the theory of np-completeness. 1979.

[11] Zoubin Ghahramani and Thomas L Griffiths. Infinite latent feature models and the indian buffet process. In *Advances in neural information processing systems*, pages 475–482, 2006.

[12] Ariel Jaffe, Roi Weiss, Shai Carmi, Yuval Kluger, and Boaz Nadler. Learning binary latent variable models: A tensor eigenpair approach. *arXiv preprint arXiv:1802.09656*, 2018.

[13] Tamara G Kolda and Brett W Bader. Tensor decompositions and applications. *SIAM review*, 51(3):455–500, 2009.

[14] Yehuda Koren, Robert Bell, and Chris Volinsky. Matrix factorization techniques for recommender systems. *Computer*, (8):30–37, 2009.

[15] Stéphane Mallat and Zhifeng Zhang. Matching pursuit with time-frequency dictionaries. Technical report, Courant Institute of Mathematical Sciences New York United States, 1993.

[16] Jan Melchior, Nan Wang, and Laurenz Wiskott. Gaussian-binary restricted boltzmann machines for modeling natural image statistics. *PloS one*, 12(2):e0171015, 2017.

[17] Pauli Miettinen. Boolean tensor factorizations. In *Data Mining (ICDM), 2011 IEEE 11th International Conference on*, pages 447–456. IEEE, 2011.

[18] Yurii Nesterov. Quality of semidefinite relaxation for nonconvex quadratic optimization. Technical report, Université catholique de Louvain, Center for Operations Research and Econometrics (CORE), 1997.

[19] Ioakeim Perros, Evangelos E Papalexakis, Haesun Park, Richard Vuduc, Xiaowei Yan, Christopher Defilippi, Walter F Stewart, and Jimeng Sun. Sustain: Scalable unsupervised scoring for tensors and its application to phenotyping. In *ACM KDD*, 2018.

[20] Piyush Rai, Changwei Hu, Matthew Harding, and Lawrence Carin. Scalable probabilistic tensor factorization for binary and count data. In *IJCAI*, pages 3770–3776, 2015.

[21] Martin Slawski, Matthias Hein, and Pavlo Lutsik. Matrix factorization with binary components. In *Advances in Neural Information Processing Systems*, pages 3210–3218, 2013.

[22] Ryota Tomioka and Taiji Suzuki. Convex tensor decomposition via structured schatten norm regularization. In *Advances in neural information processing systems*, pages 1331–1339, 2013.

- [23] Joel A Tropp, Anna C Gilbert, and Martin J Strauss. Algorithms for simultaneous sparse approximation. part i: Greedy pursuit. *Signal processing*, 86(3):572–588, 2006.
- [24] Hsiao-Yu Tung and Alexander J Smola. Spectral methods for indian buffet process inference. In *Advances in Neural Information Processing Systems*, pages 1484–1492, 2014.
- [25] Isabel Valera, Melanie F Pradier, Maria Lomeli, and Zoubin Ghahramani. General latent feature models for heterogeneous datasets. *arXiv preprint arXiv:1706.03779*, 2017.
- [26] A Jan van der Veen. Analytical method for blind binary signal separation. In *Digital Signal Processing Proceedings, 1997. DSP 97., 1997 13th International Conference on*, volume 1, pages 399–402. IEEE, 1997.
- [27] Po-Wei Wang, Wei-Cheng Chang, and J Zico Kolter. The mixing method: coordinate descent for low-rank semidefinite programming. *arXiv preprint arXiv:1706.00476*, 2017.
- [28] Eunho Yang and Pradeep K Ravikumar. Dirty statistical models. In *Advances in Neural Information Processing Systems*, pages 611–619, 2013.
- [29] Ian En-Hsu Yen, Wei-Cheng Lee, Sung-En Chang, Arun Sai Suggala, Shou-De Lin, and Pradeep Ravikumar. Latent feature lasso. In *International Conference on Machine Learning*, pages 3949–3957, 2017.
- [30] Rose Yu, Mohammad Taha Bahadori, and Yan Liu. Fast Multivariate Spatio-temporal Analysis via Low Rank Tensor Learning. In *NIPS*, 2014.
- [31] Feiyun Zhu, Ying Wang, Bin Fan, Gaofeng Meng, and Chunhong Pan. Effective spectral unmixing via robust representation and learning-based sparsity. *CoRR*, abs/1409.0685, 2014.
- [32] Feiyun Zhu, Ying Wang, Bin Fan, Gaofeng Meng, Shiming Xiang, and Chunhong Pan. Spectral unmixing via data-guided sparsity. *CoRR*, abs/1403.3155, 2014.
- [33] Feiyun Zhu, Ying Wang, Shiming Xiang, Bin Fan, and Chunhong Pan. Structured sparse method for hyperspectral unmixing. *ISPRS Journal of Photogrammetry and Remote Sensing*, 88:101–118, 2014.